International Journal of Current Engineering and Technology
E-ISSN 2277 – 4106, P-ISSN 2347 – 5161

Available at http://inpressco.com/category/ijcet

Research Article

Structural and Optical Properties of $Co_{1-x}Zn_xFe_2O_4$ Synthesis by Sol-Gel Auto Combustion Method

Inaam M. Abdulmajeed and Lana Salar. Khalil*

Physics Department, College of Science, Baghdad University, Iraq

Accepted 10 June 2016, Available online 16 June 2016, **Vol.6, No.3 (June 2016)**

Abstract

In the present work the Cobalt-zinc ferrite ($Co_{1-x}Zn_xFe_2O_4$) with x= 0, 0.25, 0.5, 0.75 and 1, were synthesized using sol-gel auto combustion method. The prepared powder showed the crystalline with a cubic spinel phase formation when examined using the X-ray diffraction (XRD) method. The particulate size, lattice parameters and X-ray density were measured for prepared samples. The Results showed that the particle size increased from (1.0) nm by increasing the Zn concentration until it reaches (2.1) nm. The lattice constant increased from (8.32071) to (8.43802) ˚A by increasing Zn^{+2} concentration, while the X-ray density decreased from (4.67412) to (4.63925) g/cm^3 during increasing of the Zn to the value (x=0.25), also decreased from (5.34513) to (5.30546) g/cm^3 by increasing zinc ion concentration to value at (x=0.75). The microstructure of the samples was studied using the Scanning Electron Microscope (SEM). Homogeneous distribution of sphere grains for $ZnFe_2O_4$.Whiskers and spheres were homogenously distributed the grain morphology changed from sphere granular to whiskers with increasing Co^{+2} content. The optical measurements showed that the ($Co_{1-x}Zn_xFe_2O_4$) thin films have direct energy gap E_g^{opt} that increases from (2.43-2.7) with the increase of Zn concentration.

Keywords: *Co-Zn ferrites; sol gel auto combustion; XRD, SEM, optical properties*

1. Introduction

In recent years, the magnetic materials have more demand in communication and information technology, because of their high frequency applications. These are very well established group of magnetic materials of the transition metal oxides which is called Ferrites [S. S. Kumbhara, 2014]. Ferrites are electrically ferrimagnetic ceramic compound materials, consisting of various mixtures of iron oxides such as Hematite (Fe_2O_3) or Magnetite (Fe_3O_4) and oxides of other metals like NiO, CuO, ZnO, MnO, CoO. The prime property of ferrites is that, in the magnetized state, all spin magnetic moments are not oriented in the same direction. Few of them are in the opposite direction. But as the spin magnetic moments are of two types with different values, the net magnetic moment will have some finite value [D. B. Fahad, 2014]. Ferrites are, like most of the other ceramics, hard and brittle [G.Sathishkumar *et al*., 2010]. The simplest among the ferrites are spinel type. Simple spinel ferrites have the general chemical formula ($M^{2+}Fe_2^{3+}O_4^{2-}$) or ($MO.Fe_2O_3$), where (M) is a divalent metal ion and the crystal structure is that possessed by the mineral spinel. Mixed spinel ferrites have the general composition ($M_{1-x}^{2}+\ B_x^{3+}\ Fe_2^{3+}O_4^{2-}$). Mixed ferrites occur when the divalent metal (M) in the formula ($MFe_2\ O_4$) is a mixture of two divalent ions or (monovalent + trivalent) ions, while still retaining the spinel structure [M. F. J. Hilli, 2008, K. J. Standley, 1972]. The spinel AB_2O_4 structure can be generally described as a cubic close-pack arrangement of oxygen ions in which tetrahedral A and octahedral B interstitial lattice sites are occupied by cations. In the normal spinel, the tetrahedral sites are occupied by divalent cations while trivalent cations occupy octahedral sites. In contrast, 2-valent cations occupy octahedral sites in inverse spinel, where a 3-valent cations are distributed equally among A- and B-sites [S. Nasrin *et al*., 2014]

2. Experimental

Ultra-fine Cobalt-zinc ferrite powder synthesized using sol-gel auto combustion method. Each one of the component ($Fe(NO_3)_3.9H_2O$), ($Co\ (NO_3)_2.6H_2O$) and($(CH_3COO)_2.Zn.2H_2O$) weighted using four digital Sartorius weighting. Using stoichiometric ratios for each component to prepare $Co_x\ Zn_{(x-1)}\ Fe_2O_4$, where X= 0, 0.25, 0.5, 0.75, 1. All of each one of the above compounds dissolved in 100 ml of deionized distilled water. The iron solution, cobalt solution and zinc solution were mixed using magnetic stirrer and so the

*Corresponding author: **Lana Salar. Khalil**

cobalt zinc ferrite solution was prepared. While the Co-Zn ferrite solution was still on the magnetic stirrer, a drops of NaOH solution was added slightly to the solution until the gel was formed. The PH of the solution was measured for all the x samples, where the gel formation begins at 8PH. Addition of citric acid that leads to hear notifying the combustion which helps in reducing the particle size of produced gel. Filtrate the solution with filter papers to get out the gel then washing it with deionized distilled water for at least three times. After filtering the gel product, dry it at 80^0 for one day in a programmed electrical oven to dry the gel. The Co-Zn ferrites powder were synthesized by ignation of gel precursor upon heating at 200 ˚C. The prepared compound crushed in a gat mortar and calcined at temperature 500°C with heating rate 5°C/min for 2 hours. The powders were finally cooled by switching off the furnace to room temperature.

3. Result and discussion

The prepared Co-Zn ferrite powders analyzed using X-ray diffraction (XRD-6000) diffract meter made in Japanese with Cu-Kα radiation (λ=1.506 ˚A) operated at voltage=40KV, current=30 mA, scanning angle (20-60), with speed=5 deg/min. The Co-Zn ferrite powder $Co_{1-x}Zn_xFe_2O_4$, where (x= 0, 0.25, 0.5, 0.75, 1) have been investigated using x-ray diffraction with a (2θ) range of about (20˚-60˚) were used for all samples in this analysis, as shown in Figures (1), (2), (3), (4) and (5).

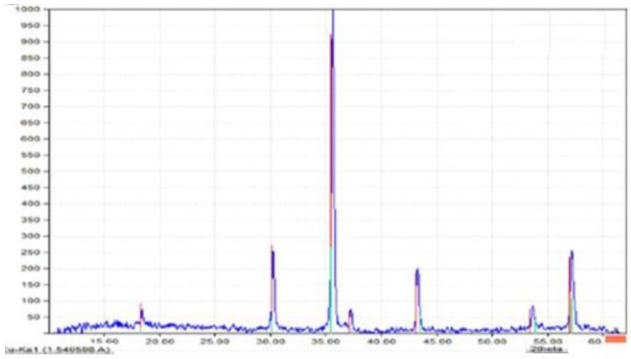

Fig.1: X-ray diffraction patterns for $CoFe_2O_4$

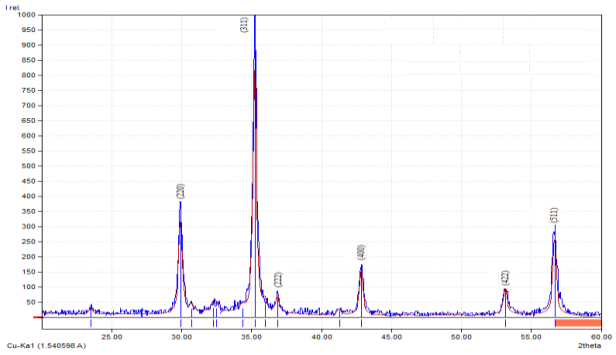

Fig.2: X-ray diffraction patterns for $Co_{0.75}Zn_{0.25}Fe_2O_4$

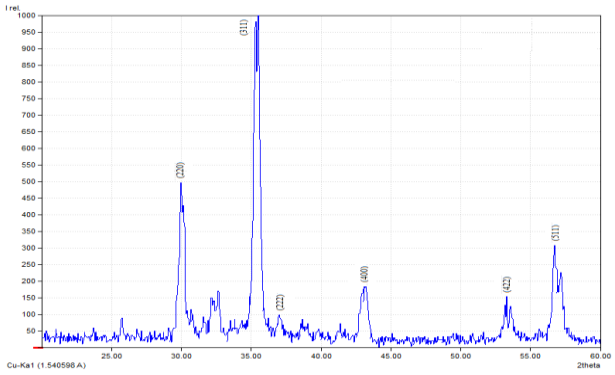

Fig.3: X-ray diffraction patterns for $Co_{0.5}Zn_{0.5}Fe_2O_4$

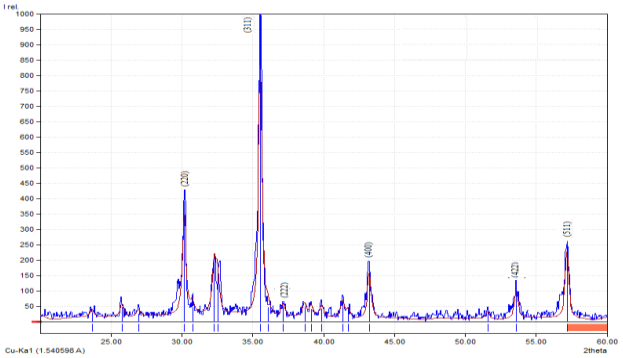

Fig.4: X-ray diffraction patterns for $Co_{0.25}Zn_{0.75}Fe_2O_4$

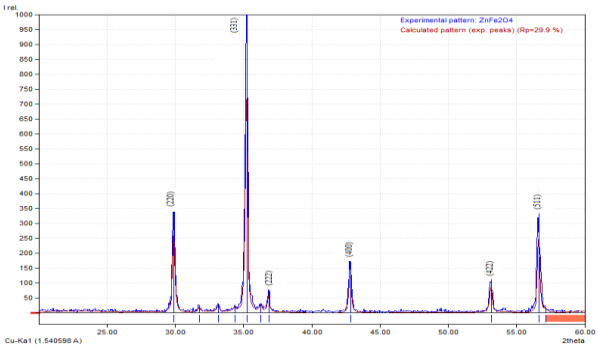

Fig.5: X-ray diffraction patterns for $ZnFe_2O_4$.

All samples were identified with JCDPS card, The diffraction peaks of all the samples are assigned to cubic spinel structure that consistent compared with the JCPDS (Joint committee on powder diffraction standard) database for phase identification of cobalt ferrite and zinc ferrite, All compositions of Co-Zn ferrites could be indexed in terms of a single phase cubic spinel structure, also It can be seen from figures that all ferrite powders showed all characteristic planes of Co-Zn spinel ferrites (220, 311, 222, 400, 422, and 511).

The average crystallite size of the samples is calculated from the diffraction peak of the (311) plane in the XRD profile, in accordance with Debye–Scherrer formula. It has been observed that the crystallite size is increase from 10.27 to 21.13 A˚ with increase in Zn content as shown in table (1).

Table1: Lattice parameters for Co-Zn ferrite with different compositions

Sample	2 theta	d (A°)	D (A°)	a(A°)	dx (g/cm³)
$CoFe_2O_4$	35.762	2.50879	10.27107	8.32071	4.67412
$Co_{0.75}Zn_{0.25}Fe_2O_4$	35.5725	2.52171	10.83161	8.36356	4.63925
$Co_{0.5}Zn_{0.5}Fe_2O_4$	35.4414	2.53074	6.08349	8.39351	5.34513
$Co_{0.25}Zn_{0..75}Fe_2O_4$	35.2685	2.54275	13.65228	8.43334	5.30546
$ZnFe_2O_4$	35.2483	2.54416	21.13186	8.43802	5.33229

It has a maximum crystallite size of 21.13 A for 1 Zn concentration, due to the larger ionic radius of Zn^{2+} ions.

The lattice constant (a) for each sample was calculated as shown in table (1). It can be seen that lattice constant of the samples increases with increasing of Zn concentration; this can be correlated with difference in ionic radii [Abdalrawf I. Ahmed, 2015]. Zinc ions have a strong tendency to be arranged at tetrahedral sites. The addition of Zn^{+2} ions into Co-ferrite structure causes migration Fe^{+3} ions from the A-site to the B- site. Zn^{+2} ions (0.83A°) owns a larger cation, as compared to Fe^{+3} ions (0.67A°) and Co^{+2} ions (0.78A°), which means that more the Zn^{2+} ion the large, the lattice parameter thus the lattice expands, this result agree with other workers [Abdalrawf I. Ahmed,2015].

The X-ray density (dx) of the ferrite powders as shown in table (1), a decreased in values from (5.33229) to (4.67412) g/cm³ as their density depend upon the lattice constant. while the lattice constant increase with the increase in Zn ion concentration.

Scanning electron microscopy (SEM) analysis model (Inspect S 50 sem) made in (USA), were performed for all the prepared samples to investigate the morphology, microstructure. The micro structure and the morphological studies of the ferrite powder were carried out using a scanning electron microscope (SEM). SEM micrographs with different magnifications (10kX and 2.5kX) for the prepared powders are shown in Figures (6) a, b, c, d, e, f. Image (6) e, showed homogeneous distribution of grains for $ZnFe_2O_4$. Whiskers and spheres were homogenously distributed the grain morphology changed from granular to wiskers with increasing Co content, Whiskers were scattered in all directions with no obvious pattern as shown in figures (6) b, c, d, also for $CoFe_2O_4$ sample as shown in fig (6) a.

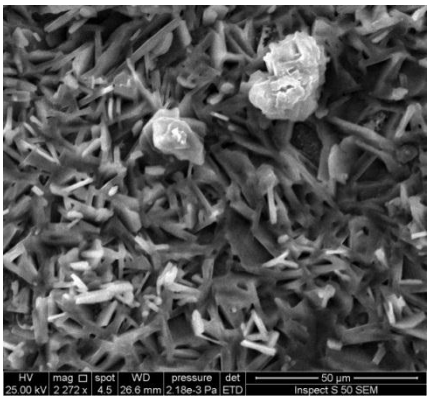

(a1)

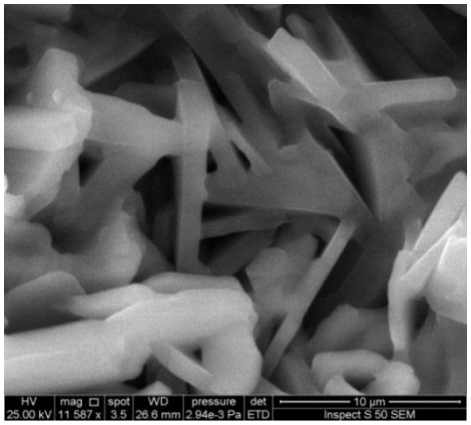

(a2)

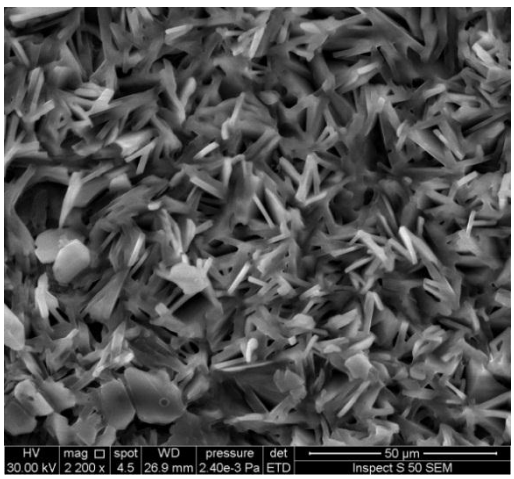

(b1)

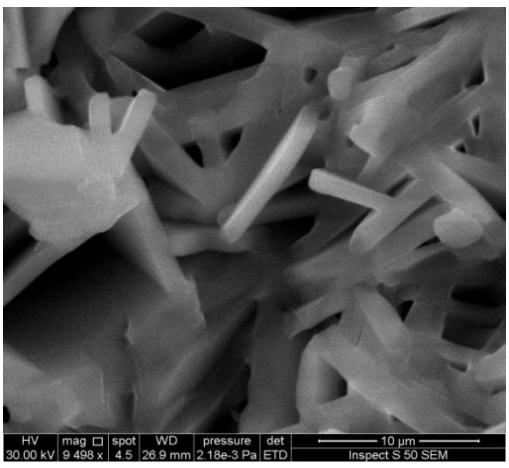

(b2)

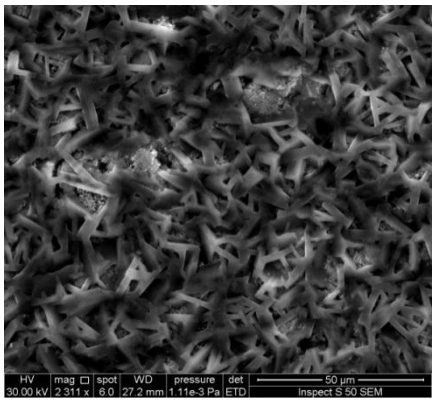

(c1)

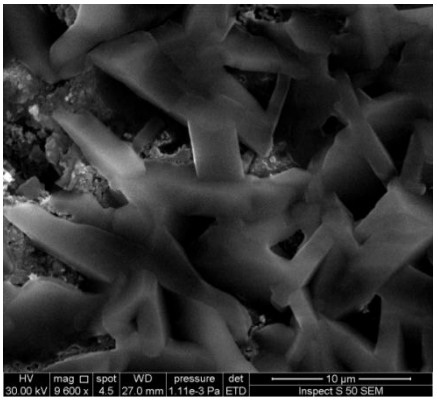

(c2)

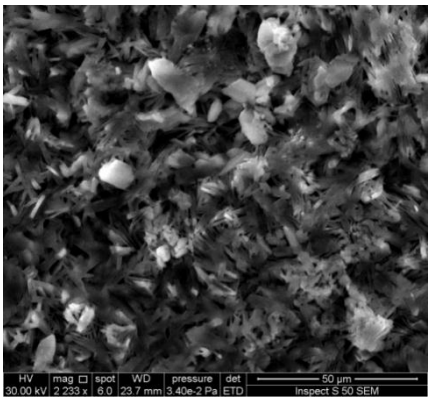

(d1)

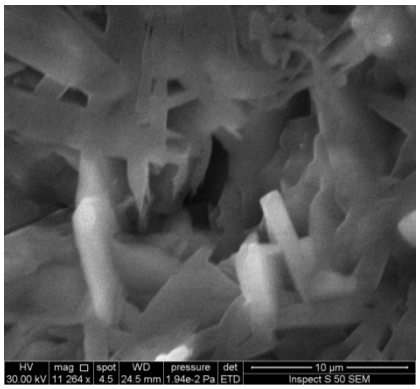

(d2)

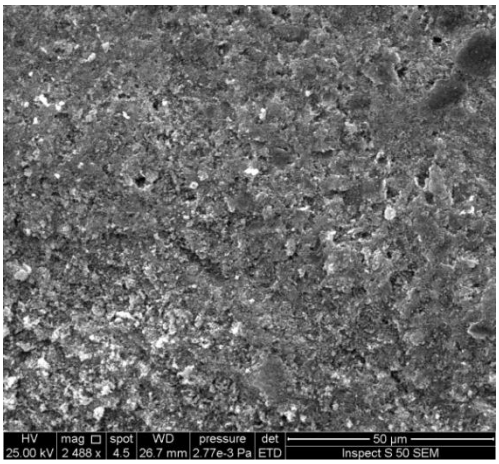

(e1)

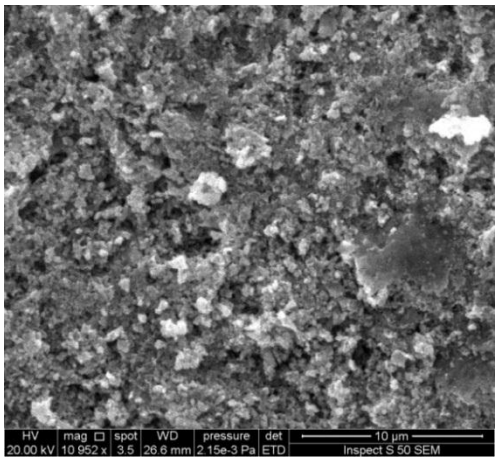

(e2)

Fig.6: The SEM micrograph for ($Co_{1-x}Zn_xFe_2O_4$) at 10kX and 2.5kX magnifications, (a, b, c, d and e) are assemble for x= (0, 0.25, 0.5, 0.75 and 1)respectively

The optical properties for the $Co_xZn_{1-x}Fe_2O_4$powder (x= 0,0.25, 0.5 0.75,1) were studied. Thin films deposited on a glass substrate for each one of composition using pulsed laser deposition(PLD) technique with power (500mJ) and no. of pulse 300 pulse, while the thickness of the prepared thin films were measured by Tolansky's interferometer method. The UV/Visible 160Shimadzu spectrophotometer was used to study the transmission spectra of the prepared samples at wavelength range (200-1100nm). The optical absorption spectrum is a significant method to attain optical energy band gap of crystalline and amorphous materials. The vital absorption, which corresponds to the electron excitation from the valance band to the conduction band, is used to verify the character and value of the optical band gap. The transmittance, absorbance spectrum, and energy gap was measured. UV- visible transmittance spectrum in the range of (200–1100) nm. The transmittance spectrum of the ($Co_{1-x}Zn_xFe_2O_4$) thin films deposited at room temperature with different (x) content are shown in Fig. (7).

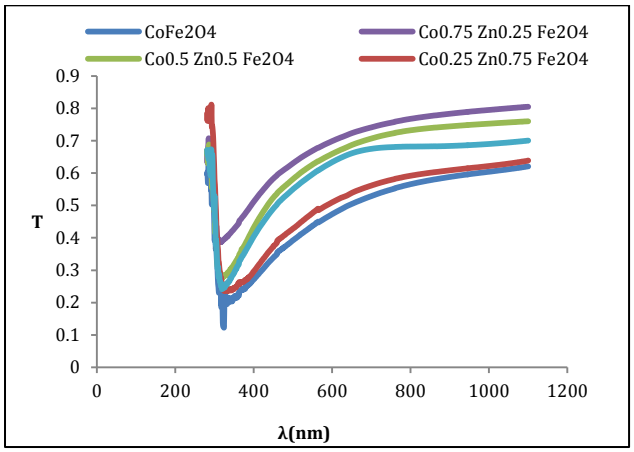

Fig.7: The transmittance versus the wavelength for Co-Zn ferrite thin films with different x content

The transmittance pattern of all deposited thin films increases with the increasing of (λ). On the other hand, the transmittance decreases with the increase of Zn content which means increase of the reflection and absorption.

The decrease of transmittance with the increase of Zn content is attributed to the increase of density due to the addition of Zn to Co and so the samples become more opaque to the incident light.

The optical energy gap values (Eg^{opt}) for deposited ($Co_{1-x}Zn_xFe_2O_4$) ferrite films for different x values were determined using Tauc equation. The analysis of the absorption coefficient in the fundamental absorption edge indicates that all the ferrite films are characterized by direct band-to-band electronic transition appearing in the photon energy range (2.43-2.7) eV.

It is found that Tauc equation yield linear dependence, which describes the allowed direct transition with r=2, respectively. Eg^{opt} is then determined by the extrapolation of the straight part at y-axis = 0 from the relations between $(\alpha h\upsilon)^2$ versus the photon energy ($h\upsilon$) as shown in Fig. (8). The band gap is affected by many factors like crystallite size, lattice parameter, and presence of impurities.

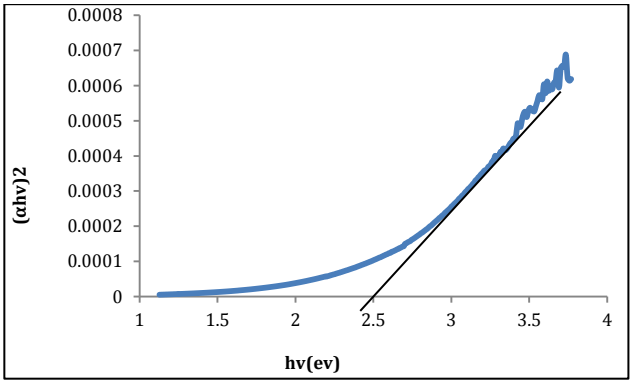

(a)

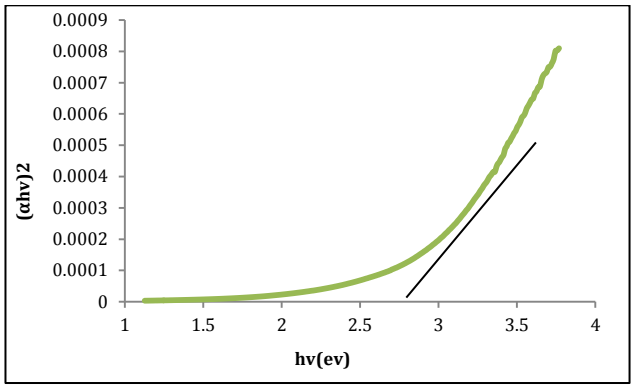

(b)

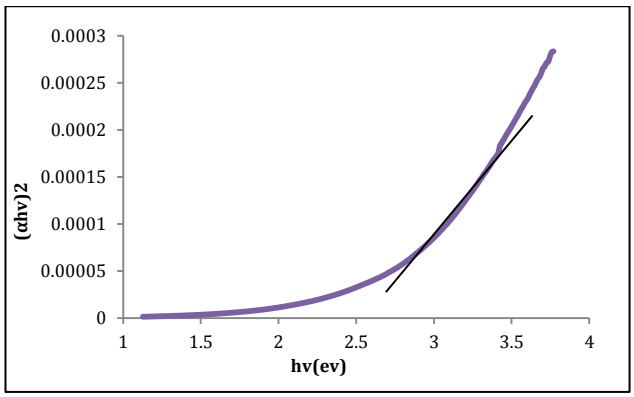

(c)

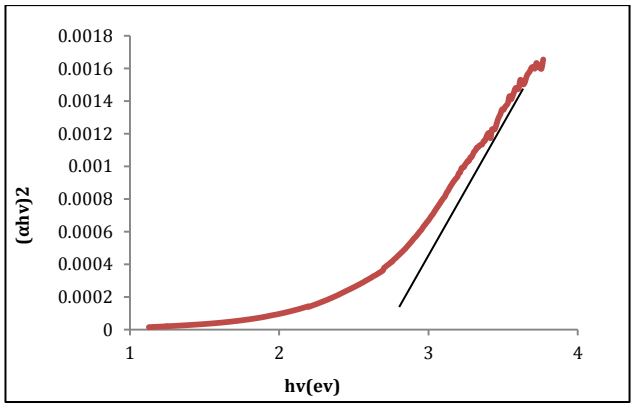

(d)

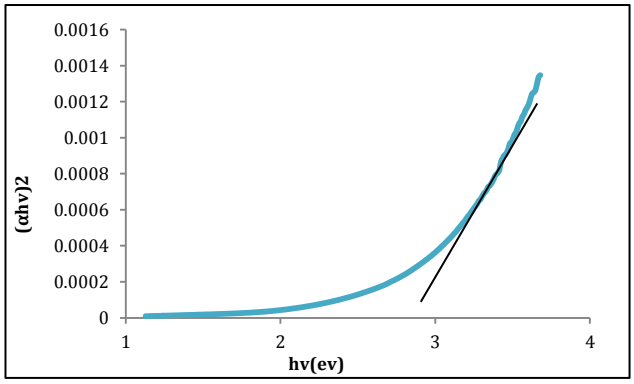

(e)

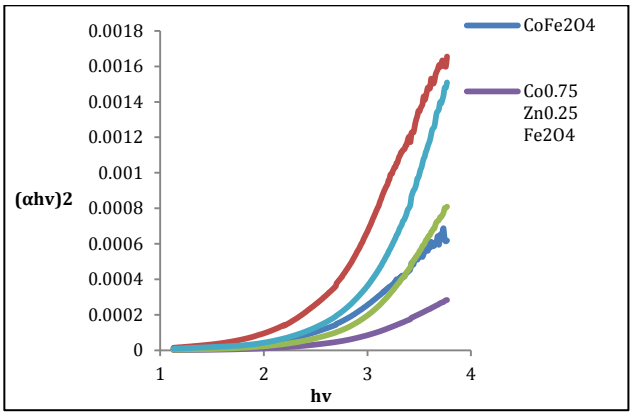

Fig.8: The variation of $(\alpha h\upsilon)^2$ versus the photon energy ($h\upsilon$) for co-zn ferrite thin films with different x content

The estimated values of direct band gap energies are listed in Table (2). The values of the direct optical energy gap, in general, increase with the increasing of the Zn contents for all sample. In the other word, the direct (Eg^{opt}) decrease from (2.7) to (2.43) eV. This is because the addition of Co causes the creation of new localized levels which are capable to receive electrons and generate localized energy tails inside the optical energy gap which work on the absorption of low energy photons (deviation of the absorption edge towards the low energies) and this in turn leads to a decrease of the energy gap localized states in the band gap which result in visual decrease of Eg^{opt} values and may be due to increase in lattice constant with Co concentration.

Table 2: The values of optical energy gap for ($Co_{1-x}Zn_xFe_2O_4$) films with different x content

samples	Optical energy gap (eV)
$CoFe_2O_4$	2.43
$Co_{0.75}Zn_{0.25}Fe_2O_4$	2.5
$Co_{0.5}Zn_{0.5}Fe_2O_4$	2.6
$Co_{0.25}Zn_{0.75}Fe_2O_4$	2.63
$ZnFe_2O_4$	2.7

Conclusions

The present work focused on the effect of different substitutions on the structural, optical and structure properties of Co-Zn ferrites. $Co_{1-x}Zn_xFe_2O_4$ ferrites with X= 0, 0.25, 0.5, 0.75 and 1. Sol-gel auto combustion is a very good method for the synthesis of ultra-fine Co-Zn ferrite particles can be achieved by suitable control of the pH of the solution. The Co-Zn ferrites powder was successfully synthesized by the ignition of gel precursor upon heating at 200°C, then calcined at 500°C. The formation of cubic spinel phase was confirmed by XRD. The lattice parameter increased from 8.32071to 8.43802 by increasing Zn^{+2} content.

SEM showed the homogenous distribution of grains with whiskers and spheres forms, the grain morphology changed from granular to whiskers with increasing Co contents. UV–Visible diffuse transmittance spectroscopy shows that the optical band gap of the synthesized pure $CoFe_2O_4$ nanoparticles is 2.43 eV and by increasing the Zn-doping, it increases to 2.7 eV. The increasing of Zn content made the prepared thin films more opaque throughout increasing the packing density and shifting the absorption edge to lower energies.

References

S. S. Kumbhara, (2014), Synthesis and characterization of spray deposited Nickel-Zinc ferrite thin films, *ScienceDirect*, Vol. 54, pp. 599 – 605.

D. B. Fahad, (2014), Structural Electric and optical properties of $CuLa_yFe_{2-y}$ Ferrite system, MSC, *University of Baghdad*.

G. Sathishkumar, C. Venkataraju and K. Sivakumar, (2010), Synthesis, Structural and Dielectric Studies of Nickel Substituted Cobalt-Zinc Ferrite, *Materials Sciences and Applications*, Vol. 1, pp. 19-24.

M. F. J. Hilli, (2008), The Effect of Preparation Conditions on the Physical Properties of Some Doped Li-Ferrites, PHD, *University of Baghdad*.

K. J. Standley, (1972), Oxide Magnetic Materials, 2nd ed., *Oxford University Press*.

S. Nasrin, S. ManjuraHoque, F.-U.-Z chowdhury and M. Moazzam Hossen, (2014), Influence of Zn substitution on the structural and magnetic properties of $Co_{1-x}Zn_x$ Fe_2O_4nano-ferrites, *Journal of Applied Physics*, Vol. 6, pp. 58-56.

Abdalrawf I. Ahmed, Mohamed A. Siddig, Abdulmajid A. Mirghni, Mohamed I. Omer, Abdelrahman A. Elbadawi, (2015), Structural and Optical Properties of $Mg_{1-x}Zn_xFe_2O_4$ Nano-Ferrites Synthesized Using Co-Precipitation Method, *Advances in Nanoparticles*, Vol.4, pp.45-52.